REPORT DOCUMENTATION PAGE

Form Approved OMB No. 0704-0188

Public reporting burden for this collection of information is estimated to average 1 hour per response, including the time for reviewing instructions, searching existing data sources, gathering and maintaining the data needed, and completing and reviewing the collection of information. Send comments regarding this burden estimate or any other aspect of this collection of information, including suggestions for reducing the burden, to Department of Defense, Washington Headquarters Services, Directorate for Information Operations and Reports (0704-0188), 1215 Jefferson Davis Highway, Suite 1204, Arlington, VA 22202-4302. Respondents should be aware that notwithstanding any other provision of law, no person shall be subject to any penalty for failing to comply with a collection of information if it does not display a currently valid OMB control number.
PLEASE DO NOT RETURN YOUR FORM TO THE ABOVE ADDRESS.

1. REPORT DATE (DD-MM-YYYY)	2. REPORT TYPE	3. DATES COVERED (From – To)
12-03-2004	Final Report	28 February 2003 - 28-Feb-04

4. TITLE AND SUBTITLE

Low-Cost Satellite Infrared Imager Study

5a. CONTRACT NUMBER
FA8655-03-1-3072

5b. GRANT NUMBER

5c. PROGRAM ELEMENT NUMBER

6. AUTHOR(S)

Dr. Craig Underwood

5d. PROJECT NUMBER

5d. TASK NUMBER

5e. WORK UNIT NUMBER

7. PERFORMING ORGANIZATION NAME(S) AND ADDRESS(ES)
University of Surrey
Guildford GU2 5XH
United Kingdom

8. PERFORMING ORGANIZATION REPORT NUMBER

N/A

9. SPONSORING/MONITORING AGENCY NAME(S) AND ADDRESS(ES)

EOARD
PSC 802 BOX 14
FPO 09499-0014

10. SPONSOR/MONITOR'S ACRONYM(S)

11. SPONSOR/MONITOR'S REPORT NUMBER(S)
SPC 02-3072

12. DISTRIBUTION/AVAILABILITY STATEMENT

Approved for public release; distribution is unlimited.

13. SUPPLEMENTARY NOTES

14. ABSTRACT

During the period of this study, the Surrey Space Centre, University of Surrey has conducted a theoretical and laboratory experiment investigation into low-cost thermal infrared imager concepts suitable for flight on very small satellite platforms. The investigation and resulting design concept(s) has emphasized the use of low-cost commercially available components while, at the same time, maximizing performance. The foundation of this research has been based on a commercially available uncooled resistive microbolometer detector array.

15. SUBJECT TERMS
EOARD, IR sensors, Space optics, microbolometer, small satellite

16. SECURITY CLASSIFICATION OF:			17. LIMITATION OF ABSTRACT	18, NUMBER OF PAGES	19a. NAME OF RESPONSIBLE PERSON
a. REPORT	**b. ABSTRACT**	**c. THIS PAGE**	UL	39	INGRID J. WYSONG
UNCLAS	UNCLAS	UNCLAS			**19b. TELEPHONE NUMBER** (Include area code) +44 (0)20 7514 4285

Standard Form 298 (Rev. 8/98)
Prescribed by ANSI Std. Z39-18

Low-Cost Satellite Infrared Imager Study
University of Surrey Project Ref. 107627

UNIVERSITY OF SURREY 12-MONTH DELIVERABLE: FINAL REPORT

SUBMITTED DATE: 1 March 2004

SUBMITTED BY: Dr. Craig Underwood
Principal Investigator
Surrey Space Centre
University of Surrey
Guildford, Surrey GU2 7XH

INTRODUCTION

This report contains the information required for the final deliverable, of EOARD Grant/ Cooperative Award number FA8655-03-1-3072 (University of Surrey Project Reference 107627). As specified in the agreement, this report contains a summary of research efforts and final conclusions resulting from the effort of this 12-month study. More specifically, this report and its attachments will summarize the findings of Research Tasks 1 through 7 presented in the work breakdown structure in the 1 month deliverable, PRELIMINARY REPORT. There are no changes to the research summary, research objectives, and the work breakdown structure presented in deliverable 1 but they are presented again here for completeness.

RESEARCH SUMMARY

During the period of this study, the Surrey Space Centre, University of Surrey has conducted a theoretical and laboratory experiment investigation into low-cost thermal infrared imager concepts suitable for flight on very small satellite platforms. The investigation and resulting design concept(s) has emphasized the use of low-cost commercially available components while, at the same time, maximizing performance. The foundation of this research has been based on a commercially available uncooled resistive microbolometer detector array.

RESEARCH OBJECTIVES

The following is a list of the research objectives presented at the beginning of this study:

- Survey the spaceborne thermal infrared imaging field. Document existing and emerging mission areas and requirements for thermal infrared data.
- Survey commercially available imager components to include detectors, calibration sources, optics, and electronics. Determine the best value for imager performance.

- Acquire representative imager components and characterize within a laboratory environment
- Utilize test data to assemble a valid low-cost imager concept(s) with a high certainty of useful performance on a small satellite platform.

WORK BREAKDOWN STRUCTURE

In order to complete these objectives, the following work breakdown structure has been applied. Is has been designed as a guidance tool only as was subject to change with the uncertainties inherent in applied scientific research. This report will summarize the findings of these tasks.

Task No.	Task Name	Completion Date
1	Survey thermal infrared satellite mission areas (existing and emerging)	1 April 2003 ✔
2	Survey Commercially available detector arrays	1 May 2003 ✔
3	Complete preliminary imager design	1 June 2003 ✔
4	Acquire basic components for laboratory evaluation	1 Aug 2003 ✔
5	Characterize components	On-going
6	Complete final imager concept design(s)	1 Feb 2004 ✔
7	Final documentation	1 Mar 2004 ✔

FINAL STATUS OF RESEARCH TASKS

TASK 1 STATUS:

Task Name: Survey thermal infrared satellite mission areas (existing and emerging)
Completion Date: 1 April 2003

Task Description: In this task, a review of Earth observing satellite instruments operating in the thermal (mid-wave and long-wave) infrared (3 –5 and 8 – 14 μm spectral ranges respectively) was completed using open sources. The satellites were catalogued and their prime mission have been summarized. In addition, a cursory look at emerging mission areas was noted and a final mission requirements list was documented. Focus has been on global change and environmental/disaster monitoring.

Status: Complete. See Report in Attachment 1.

TASK 2 STATUS:

Task Name: Survey commercially available detector arrays
Completion Date: 1 May 2003

Task Description: Given that the imager concept design(s) will be built around a commercially available detector array, it has been the focus of the component investigation. In this task, the limits of detector size, pixel pitch, detectivity, and integration time were defined as well as delivery time times and costs of those detectors identified as candidates for laboratory characterization.

Status: Complete. See Report in Attachment 2.

TASK 3 STATUS:

Task Name: Complete preliminary imager design
Completion Date: 1 Jun 2003

Task Description: With a candidate detector array identified, the component survey was completed with a look at available optics, calibration sources, and electronics. From this, a preliminary imager concept has been designed and its theoretical on-orbit performance evaluated using a radiometric model.

Status: Complete. See Report in Attachment 3.

TASK 4 STATUS:

Task Name: Acquire basic components for laboratory evaluation
Completion Date: 1 Mar 2004

Task Description: Selected components (within the allowable cost budget defined in the agreement), to include detector arrays, optics, back body sources, and electronics have been ordered for delivery to the Surrey Space Centre.

Status: Complete. All funds allocated for equipment has been committed. See summary of equipment purchased in Attachment 4.

TASK 5 STATUS:

Task Name: Characterize components
Completion Date: On-going

Task Description: This task involves the bench top evaluation of all candidate components acquired in task 4. This includes a detector characterization (e.g. relative spectral response, NETD, time constant, etc.), optics characterization (e.g. thoughput, MTF, etc.), and overall system performance (e.g. calibration, imaging thermal scenes, etc.).   Relevant data will be documented and integrated back into the final imager design(s).

Status: On-going. Surrey Space Centre took delivery of the prime imager components on 18 Feb 04. Therefore, there has not been ample time to collect the data specified in this task. However, **although not a requirement in the original agreement**, the data and conclusions derived from the data will courtesy copied to EOARD once they become available (approx. Apr/May 04).

TASK 6 STATUS:

Task Name: Complete final imager concept design(s)
Completion Date: 1 February 2004

Task Description: A final imager concept was designed and is presented in Attachment 5. This has been possible by working closely with the uncooled microbolometer vendor (ULIS)

on developing an accurate prediction of Earth observation performance. Surrey Space Centre specialists were consulted on technical interface requirements imager integration on a small satellite platform. The final design, the imaging concept, and its expected performance have been documented.

Status: Complete. See Attachment 5.

TASK 7 STATUS:

Task Name: Final documentation
Completion Date: 1 March 2004

Task Description: The information gathered in the previous 6 tasks has been compiled, reviewed, and documented in a final report and is now delivered (Final Report) to the USAF EOARD.   This Final Report and its attachments have detailed all research completed on state-of-the-art uncooled IR imager technologies, a trade study on available IR imager COTS hardware/software, and, of course, the final imager design.

Status: Complete. See this report and attachments.

CONCLUSION

This final report has summarized the findings of tasks 1 through 7 of the work required by EOARD Grant/Cooperative Agreement Award FA8655-03-1-3072. If there are any questions or comments regarding the content of this report, they should be directed to Dr. Craig Underwood at C.Underwood@eim.surrey.ac.uk or Brian Oelrich at B.Oelrich@sstl.co.uk.

EOARD Grant/Cooperative Agreement Award
Award No. FA8655-03-1-3072
Low-Cost Satellite Infrared Imager Study
University of Surrey Project Ref. 107627
UNIVERSITY OF SURREY DELIVERABLE 2: ATTACHMENT 1 (OF 5)
TASK 1: SURVEY THERMAL INFRARED SATELLITE MISSION AREAS

1.0 INTRODUCTION

In preparation of the design of a low-cost thermal IR imager for a microsatellite, a survey of past, existing, and planned thermal infrared (TIR) imaging missions was taken. In order to set the stage for what imagers have flown and their TIR imaging characteristics, it is first necessary to define exactly what is the TIR and what they tell the data user. This will be done in the next two sections. Then, a compilation of the current field in TIR imaging satellites will be presented followed by an analysis and problem statement for which this research programme has been based.

2.0 DEFINING THE TIR

The TIR has long been of interest for space-borne remote sensing. This region of the electromagnetic spectrum is dominated by two distinct bands, hereafter known as the mid-wave infrared (MWIR) and the long-wave infrared (LWIR), (the latter sometimes referred to as the far-infrared), correspond roughly to the atmospheric windows at 3 –5 μm and 8 – 12 μm light waves respectively and each contain useful information about the scene from which they radiate. Imaging in these two wavebands is unique in that they involve the sensing of radiant (thermal) energy of the scene as opposed to reflected solar energy as is the case for traditional imaging in the ultra-violet (UV), visible (VIS), and near infrared (NIR). All objects above absolute zero emit thermal energy and in the MWIR and LWIR, this energy far exceeds any reflected solar energy. This concept can be better understood by examining Planck's radiation law[1] for blackbody radiation which is stated by

$$W_\lambda = \frac{C_1}{\lambda^5 [e^{C_2/\lambda T} - 1]} \tag{1}$$

where W_λ is the spectral irradiance (W cm^{-2} μm^{-1}), λ is the wavelength (μm), T is the blackbody temperature (K), C_1 is 37,418, and C_2 is 14,388. To illustrate the nature of MWIR and LWIR radiation, the spectral irradiance values described by Planck's radiation law for the following blackbody temperatures has been calculated yielding the following characteristics.

Table 1: Spectral radiant wavelength and peak emittance values for various blackbody temperatures

	Black-body Temp (K)	λ$_{peak}$ (μm)	W$_{λmax}$ (Watt cm^{-2} μm^{-1})

From table 1, the types of missions targeted by traditional MWIR and LWIR imaging missions becomes apparent. The MWIR is best used to discriminate hot spot events such as vegetation fires or erupting volcanoes and the LWIR is best used to image thermal contrasted scenes in the 300 K range. As previously mentioned, the UV, VIS, and NIR are best used to image reflected solar energy, which dominates in these wavebands.

3.0 THE UTILITY OF SPACEBORNE MWIR AND LWIR IMAGERY

For the remote sensing user community, there are numerous applications for data describing the MWIR and LWIR radiation of an Earth ground scene. By mapping spatial flux and emissivity difference across the scene, various missions have been established. The following lists compiled from various spacecraft mission websites[2-4] includes some of the more prominent mission areas and the following figure shows two examples of MWIR and LWIR imaging products.

3.1 Mid-wave Infrared Imaging Missions (3 –5 um):
- Vegetation fire detection, location, characterization, and monitoring
- Volcanic eruption monitoring
- Detect/monitoring burning oil wells and coal seams

3.2 Thermal Infrared Imaging Missions (8 – 12 um):
- Sea surface temperature (ocean current mapping, weather prediction)
- Sea ice mapping (collision avoidance and environmental change monitoring)
- Cloud top temperature and height, cloud cover extent (weather prediction)
- Land surface temperature & emissivity (vegetation type, land use, urban islands, etc.)
- Snow and ice (glacial, polar, etc.) cover extent
- Soil and vegetation moisture level
- Aerosol and atmospheric water vapour measurements
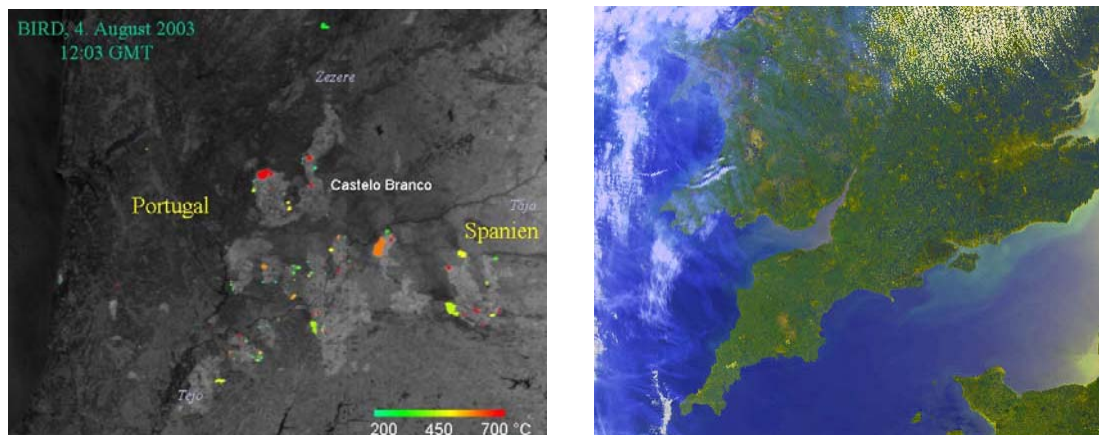- Volcanic plume imaging

Figure 1: MWIR and TIR satellite imagery. On the left is a BIRD image of forest fires on the Portuguese/Spanish border[3] and the image on right is from AATSR of the English Channel[4].

4.0 THE CURRENT FIELD OF MWIR AND LWIR IMAGING MISSIONS

The following table[2] lists several representative Earth observation payloads utilizing the MWIR and LWIR either currently on-orbit or planned to be launched in the near future. The list is my no means exhaustive but illustrates the mainstream approach to instrument design for meeting the mission requirements summarized in the previous section.

Instrument	Wavebands	Instrument Mass	GSD	Swath	Orbit Altitude
Advanced Along-Track Scanning Radiometer (AATSR)[*]	VIS, NIR, SWIR, MWIR, LWIR	101 kg	1 km	500 km	782 km
Advanced Spaceborne Thermal Emission and Reflection	VIS, NIR, SWIR, LWIR	450 kg	90 m	60 km	705 km

Radiometer (ASTER)[†]					
Along Track Scanning Radiometer – 2 (ATSR-2)[‡]	VIS, NIR, SWIR, MWIR, LWIR	not available	1 km	500 km	782 km
Advanced Very High Resolution Radiometer/2 (AVHRR/2)[§]	VIS, NIR, MWIR, LWIR	33 kg	1.1 km	3000 km	845 km
MWIR and LWIR Channels (BIRD)[**]	VIS, NIR, MWIR, LWIR	26 kg	290 m	148 km	500 km
Enhanced Thematic Mapper + (ETM+)[††]	VIS, NIR, SWIR, LWIR	425 kg	60 m	185 km	705 km
Global Imager (GLI)[‡‡]	VIS, NIR, SWIR, MWIR, LWIR	not available	1 km	1600 km	803 km
Moderate-Resolution Imaging Spectro-Radiometer (MODIS)[†]	VIS, NIR, SWIR, MWIR, LWIR	229 kg	1 km	2330 km	705 km

Notes:
* European Space Agency (ESA) instrument flown on Envisat in 2002.
[†] NASA and Japanese instrument flown on Terra in 1999.
[‡] ESA instrument flown on ERS-2 in 1995
[§] National Oceanic & Atmospheric Admin (NOAA) instrument flown on NOAA-11-16 in 1998.
[**] German Aerospace Center (DLR) instrument flown on Bi-spectral Radiometer (BIRD) in 2001.
[††] NASA instrument flown on Landsat-7 in 1999.
[‡‡] NASDA (Japan) instrument flown on ADEOS-2 in 2002.

Table 2: Representative MWIR and TIR instruments in the current field

In order to better understand what the resolution and ground coverage requirements are for a candidate TIR instrument, the following plot of swath width verse ground sample distance (GSD) was created.

Swath Width (km)

500   MUST, GLI   MODIS   AVHRR/3
                                                    AATSR   ATSR-2
400

300

200   ETM+   BIRD
                       FEUGO
100

       ASTER

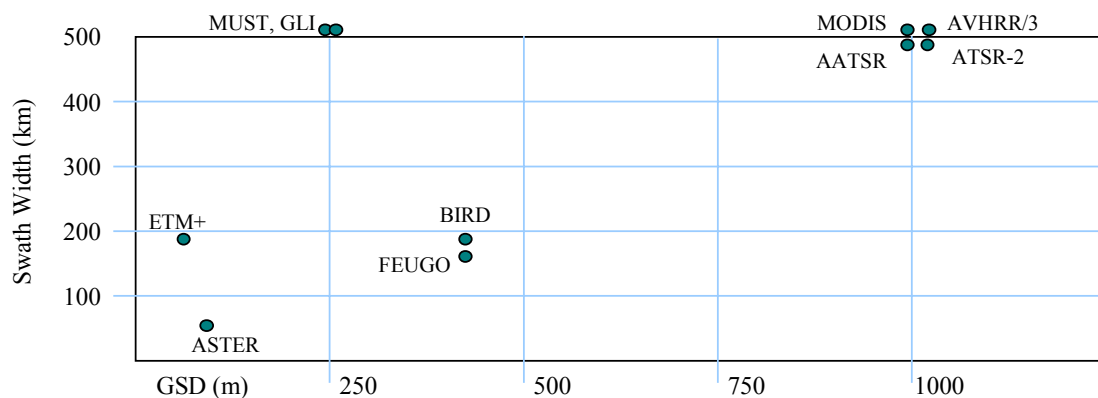GSD (m)   250   500   750   1000

Figure 2: Swath Width vs. GSD for major space-borne MWIR and TIR imaging instruments

Expanding this presentation of the current field, two representative instruments have been selected for closer examination. Those instruments are ESA's AATSR and DLR's BIRD and together, they adequately represent the spectrum of existing instruments built to address the range of MWIR and LWIR imaging requirements.

4.1 Advanced Along-Track Scanning Radiometer (AATSR)

AATSR is one of many payload on the ESA Envisat satellite which launched in 2002[4]. The prime mission for AATSR is to perform precise thermal mapping of the Earth's surface for a variety of user communities. AATSR is typical of large-scale heritage MWIR/LWIR missions in that it utilizes a scanning mirror, which scans the ground scene as the spacecraft flies overhead (wiskbroom). A sample of an AASTR data product (image) has been shown in figure 1. The following table and illustration describe AASTR in more detail.

Spacecraft Parameter	Value
Spacecraft mass	
Payload mass	
Pointing accuracy	
Orbit altitude	
Imager Parameter	
Waveband (MWIR)	
Waveband (TIR)	
Quantization	
Ground pixel size	
Swath width	
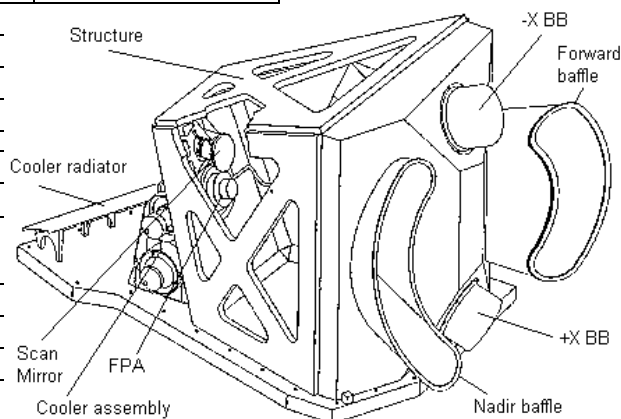
Data rate	1 Mbps
NETD at 270 K	0.05 K

Table 3: Characteristics of AATSR   Figure 2: AATSR

AATSR has been very successful in the performance of its design mission but is limited in temporal coverage by the nature of flying on a spacecraft in single low earth orbit.

4.2 Bi-Spectral Infrared Radiometer (BIRD)

The main payload of DLR's BIRD micro-satellite is a dual channel instrument for MWIR and LWIR imagery based on cooled HgCdTe (MCT) line detectors[3]. Although the imaging payload is heavy for micro-satellite standards, it was successfully integrated on a micro-satellite taking up 30 percent of the entire 92 kg spacecraft mass. The key mission objective of BIRD during it's one year mission life, which began in October of 2001, was hot spot recognition. During this time, high quality imagery of forest fires, volcanoes, and burning coalmines was taken allowing for precise hot spot characterization (hot spot size, temperature, and location). A sample of a BIRD data product has been shown in figure 1. The following table and illustration describes the BIRD MWIR and TIR payload.

Spacecraft Parameter	Value
Spacecraft mass	85 kg
Payload mass	26 kg
Pointing accuracy	0.5' per axis
Orbit altitude	500 km

Imager Parameter	Value
Waveband (MWIR)	3.4 - 4.2 μm
Waveband (TIR)	8.5 - 9.3 μm
Quantization	16 bit
Ground pixel size	290 m
Swath width	148 km
Data rate	420 kbps
Min resolvable 800K fire	$100 - 280$ m^2

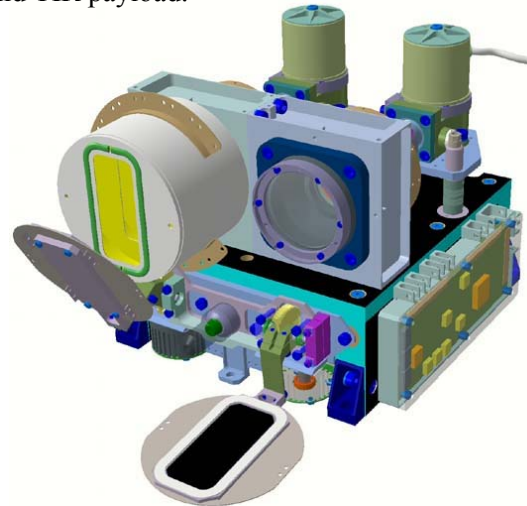Table 4: Characteristics of BIRD   Figure 3: BIRD

The BIRD hot spot recognition system made several advances in the miniaturization of infrared imagers for small satellite platforms including the integration of the detector/cooler assembly. In addition, the radiometric performance for hot spot detection rivals any of that for larger and more costly systems flown in the past. However, although the instrument is small enough to fly on a microsatellite, and hence much less expensive to place on orbit, it still is considered a high cost system utilizing government supplied detector arrays and coolers. Moreover, given that BIRD was a technology demonstration satellite, it lacked the temporal resolution to meet most fire detection time requirements. Whether a hot spot detection constellation using BIRD technology is affordable is to be determined.

5.0 RECENT ADVANCES IN MINIATURIZATION: UNCOOLED TECHNOLOGY

In effort to reduce the mass, bulk, and cost of space-borne MWIR and TIR imagers, instrument engineers are continually evaluating advances in the miniaturization of detector technology. One significant technology trend has been advances uncooled microbolometer arrays which still lag radiometrically behind cooled technology but offer significant savings in cost, mass, and size. Because this closely follows the direction of this research program the following section will summarize the proposed use of this technology.

5.1 Uncooled Infrared Spectral Imaging Radiometer (ISIR)

In August 1997, the infrared spectral imaging radiometer (ISIR) based on uncooled microbolometer technology and built by Goddard Flight Centre, was flown on space shuttle mission STS-85[5]. The ISIR instrument provided 250 m sample distance at four TIR wavelengths (using a filter wheel) selected for cloud remote sensing. A major goal of the work was to develop compact and less costly cloud imagers for small satellite missions. The detector array was government furnished and manufactured by Loral in the United States.

5.2 MediUm scale Surface Temperature (MUST) Instrument

In 1997, Matra Marconi Space and their partners completed a study sponsored by the European Commission (DG XII) for a large swath, medium resolution thermal infrared instrument called MUST[6]. The basis of their design was a series of custom uncooled microbolometer arrays manufactured by INO in Canada (see section 4.1.4.2). Although they utilized uncooled technology, the required GSD and swath width, in addition to a sophisticated calibration method resulted in a fairly heavy instrument (60 kg). However, the MUST instrument was originally designed for flight on SPOT 5 and therefore was not intended to be microsatellite compatible. No documentation has been found as to the actual flight of this instrument concept.

5.3 TIR Channel (FEUGO)

In 1998, the European Commission (DG XII) again commissioned a study, this one called FUEGO2[7]. Several agencies took part in the FEUGO2 contract to develop VIS, NIR, MWIR, and LWIR imaging cameras to be used in a 12-satellite constellation designed to detect forest fires. The LWIR camera was designed by Alcatel Space and was based on a French manufactured ULIS 240 x 320 uncooled microbolometer array. Although the TIR camera design was microsatellite compatible, it was part of a bulky and prohibitively expensive satellite and constellation design. These high costs were one of the contributions to the cancellation of the FEUGO program in 2003.

In summary, the following table lists the key parameters of the three TIR imagers, based on uncooled detector technology described above.

Parameter	ISIR	MUST	FUEGO (TIR)
Spacecraft mass	N/A (Shuttle)	SPOT	275 kg
TIR Payload mass	13 kg	60 kg	4.1 kg
Orbit altitude	250 km	SPOT	700 km
Wavebands (TIR)	8.2 – 9.0, 10.3 – 11.3, 11.5 – 12.5, and 8 – 12.5 μm	10.3 – 11.3 and 11.2 – 12.2 μm	8 – 12 μm
Focal length	50.8 mm	115 mm	60 mm
f-number	f/0.73	f/1	f/1.15
Detector	Loral VOx Microbolometer array (government furnished)	INO VOx Microbolometer array (custom fabricated)	ULIS 240 x 320 a-Si Microbolometer array
Pixel Size	50 μm	35 μm	45 μm
Pixel Count	327 x 240	2 x 1536 (3 arrays)	2 x 240 (320 x 240 array)
Dynamic Range	not available	250 – 350 K	240 – 380 K
Quantization	12 bit	12 bit	12 bit
Ground pixel size (nadir)	250 m	250 m	369 m
Swath width	82 km	1420 km	177 km
Power Consumption	20 W	100 W	22 W
Data rate	368 Kbps	3.5 Mbps	167 Kbps

| NETD @ 300 K | 0.1 K | 0.43 K | 0.33 |

Table 5: Summary of proposed TIR imagers using uncooled microbolometers

6.0 ANALYSIS

6.1 Advantages of the approaches taken to date

Obviously, there have many significant contributions by these heritage and recently proposed MWIR and LWIR Earth observation (EO) satellite systems. After all, this branch of the remote sensing community is well established and the field has been well researched and refined by numerous satellites missions exploiting the information contained in TIR data. The keys advantages to the approaches taken by the current field are summarized as follows:

- **Well grounded to the TIR data user community**; data products are well known and effectively distributed to a variety of scientific and operational users.
- TIR instruments are of **high quality** pushing the limit of what is physically possible with regards to spatial and spectral/thermal resolution.

6.2 Shortfalls of the approaches taken to date

However, there are well-recognized limits to the current field of instruments despite the advantages above. Most of the shortfalls are inherent to most instruments commissioned by large, national space agency sponsored missions. These shortfalls are summarized as follows:

- **Dependence on restrictive, government-owned detector technology.** Nationally sponsored TIR EO missions typically have access to restrictive, government-owned detector technology, which as a rule, usually offers the highest performance. Therefore, there are few designs based on COTS detectors.
- Large-scale TIR EO missions, demanding top performance and a high reliability lead to **large, complex, and costly** instruments with built-in redundancies and **long development timelines**. This covers all the systems listed in this literature review.
- Strongly associated with the previous comment is the inherent **lack of temporal frequency** of instruments flying on single platforms. The solution of flying a constellation of satellites to increase the ground repeat time of an imager is just not affordable.
- Lastly, the scale and investment requirements described above often require a **generalization of mission requirements** to serve the largest set of users as possible to justify the cost. Therefore, specialized data sets (i.e. custom spatial, spectral, or temporal resolutions) are usually not possible.

7.0 CONCLUSION

In summary, the following problem statement can be made about the nature of past and current approaches to thermal IR EO instruments and will be the focus of this EOARD sponsored research study:

Problem Statement: High temporal frequency (with a reasonable spatial and spectral resolution) and highly customized instrument design (as might be required from a niche TIR data user) are not currently feasible with the current approach to T IR EO systems. The key barriers being their high cost and size as well as their dependence on government provided hardware.

REFERENCES

1. Riedl, Max J., *Optical Design Fundamentals for Infrared Systems*, SPIE Press, 2001, pp 5.

2. ESA EO Handbook,
http://www.eohandbook.com/ceos/pdf/satellite_missions.pdf/satellite_instruments.pdf .

3. DLR Bird Website, http://spacesensors.dlr.de/SE/bird/3-0scientific.html .

4. AATSR Website, http://envisat.esa.int/dataproducts/aatsr/CNTR3-1-
2.htm#eph.aatsrinst.instdesc.instfunc .

5. Spinhirne, James D., et. al., *Preliminary Spaceflight Results from the Uncooled Infrared
Spectral Imaging Radiometer (ISIR) on Shuttle Mission STS-85*, available at
http://isir.gsfc.nasa.gov .

6. Olivier Saint-Pé, et. al., *Study of an Uncooled Focal Plane Array for Thermal Observation
of the Earth*, Proceedings of SPIE Vol. 3436, 1998, pp. 593.

7. Geoffray, Hervé, et. al., *Measured Performance of a Low Cost Thermal Infrared
Pushbroom Camera Based on Uncooled Microbolometer FPA for Space Applications*,
Proceedings of SPIE Vol. 4540, 2001, pp. 298.

EOARD Grant/Cooperative Agreement Award
Award No. FA8655-03-1-3072
Low-Cost Satellite Infrared Imager Study
University of Surrey Project Ref. 107627
UNIVERSITY OF SURREY DELIVERABLE 2: ATTACHMENT 2 (OF 5)
TASK 2: SURVEY COMMERCIALLY AVAILABEL DETECTOR ARRAYS

1.0 INTRODUCTION

The traditional development approach for Earth observation (EO) satellite payloads has been to start with a set of well defined mission requirements, and then either to apply existing or create new technology to meet these requirements. This approach may be appropriate for large-scale satellite programs, where scientific and monetary resources permit. However, this approach is less practical for small satellite programs, where low-cost and rapid engineering timescales are major mission drivers. Here, it is often the immediate availability of commercial-off-the-shelf (COTS) technology, which drives many of the advances in instrument design. Thus, by leveraging off the commercial demand for certain technologies (usually designed for terrestrial applications), the development costs, risks, and time requirements can be reduced significantly. Therefore, for this study, a survey of low cost COTS technologies has been carried out, prior to defining final mission requirements. In reality, the mission definition and the technology survey occur simultaneously and are iterative.

2.0 COOLED VS. UN-COOLED TECHNOLOGY

In the development of any EO imager, it is the choice of detector array that drives the ultimate capability of the system. Therefore the focus of our COTS survey, which encompasses optics, electronics, etc., has been the infrared detector array. The survey's goal has been to find candidate commercially available detector arrays that offer the best performance in terms of weight, size, power consumption, and cost.

Obviously, recent advances in un-cooled TIR detector technology are an attractive starting point in the design of a low-cost/mass instrument. However, although Surrey is not the first to propose the use of un-cooled detectors for space-based EO missions (see attachment 1), this is still a departure from the mainstream use of cooled photon detectors for space instruments. Therefore, it is important to understand the rationale for abandoning the "tried and tested" technology of the past, which still offers the best radiometric performance, and which has also advanced considerably over the past several years. The TIR EO designer has a variety of cooled technologies to choose from, including field proven HgCdTe (MCT) detector arrays, antimonide-based materials, and quantum well infrared photodetectors (QWIP). However, in this study, we are looking for an order of magnitude decrease in mass and cost - moving to approximately the 1-5 kg mass range, and less than $50K cost – whilst still achieving reasonable mission utility.

It should be noted that the required concessions made in radiometric performance for un-cooled technology have been dramatically reduced in recent years. Un-cooled TIR detectors have been around for decades but due to leaps in micromachining and thin-film deposition technologies, developers have now been able to create arrays of very small and thermally isolated pixel structures compatible with silicon IC processes. These advances, in addition to the integrating of the detector electronics at the sensor head, has created an un-cooled detector array industry offering a wide variety of very small 320 x 240 pixel devices, with reported noise equivalent temperature differences (NETDs) less than 100 mK. It is this growing

commercial industry that we will leverage in our TIR imager development. Cooled TIR technology may eventually become part of Surrey's EO payloads, but, for the reasons outlined above, un-cooled detectors have become a practical first step to image in the TIR band.

3.0 SURVEY CRITERIA

Since commercial un-cooled technology presents fundamental limitations in radiometric performance, it is important to choose a state-of-the-art device. In the development of our imager concept, the following basic selection criteria were applied to selecting an un-cooled detector array:

- responsiveness in the infrared corresponding to the TIR atmospheric windows (i.e 3 – 5 μm and 8 – 12 μm);
- large array size (large pixel count, small pixel pitch, high pixel fill factor);
- good radiometric performance, i.e. small noise equivalent temperature difference (NETD) and high responsivity
- small thermal time constant (to prevent pixel blur from imaging from a moving spacecraft);
- small size, weight, and power consumption (integrated read out integrated circuit (ROIC), thermal stabilizer, packaging, chopper requirement, etc.);
- cost of both detector and support electronics;
- commercial availability (reasonable production line, non-prohibitive export controls, delivery times);
- vendor's propensity for future technology advances and product availability.

4.0 CHOICES IN UN-COOLED TECHNOLOGY

In this survey the three main classes of un-cooled infrared technology (pyroelectric, thermoelectric, and resistive bolometer) were initially evaluated. Whilst pyroelectric arrays were found to have strong potential for EO, the fact that they require a mechanical chopper, and hence have the potential for inducing micro-vibrations on very small satellite platforms, made them unattractive in light of alternative technologies. Thermoelectric arrays also offered some potential, but the technology still requires significant development in the commercial sector. We note, however, that there have been some advances in thermoelectric arrays, which holds potential for Sun or Earth sensors for spacecraft attitude determination. Commercial array sizes and radiometric performance are improving, and so SSC will continue to closely monitor thermoelectric arrays.

The last class of un-cooled infrared technology, resistive bolometers, has recently been the most aggressively developed of the three for terrestrial applications. Resistive bolometers have been around for decades, but it has been the recent developments mentioned in section 2.0 that has led to a surge in commercially available microbolometer arrays. These arrays are finding multiple markets in fire fighting, security, and manufacturing, which encourages streamlined production processes and increasingly less expensive and better performing devices. In the next section, a summary of commercially available microbolometer arrays will be presented.

4.1 Commercially available resistive microbolometer arrays

The typical commercially available microbolometer array has the following characteristics: 320 x 240 pixel array, 35-50 μm pixel pitch, and an NETD less than 100 mK at 300 K with f/1 optics. However, international competition is growing and subtle variations are common and will be outlined in this section.

4.1. 1 United States

One of the leading sources of commercial microbolometers is in the United States, where pioneering microbolometer development began in 1982, primarily supported by military funding.[1] Vanadium Oxide (VOx) currently dominates as the bolometer material of choice. It was chosen early on for its high thermal coefficient of resistance (TCR) and compatibility with silicon IC technologies. The US microbolometer industry has various respectable commercial arrays with performance specifications at the top of the international market. However, heavy export controls make the majority of these arrays difficult to obtain outside the United States.

4.1..2 Canada (INO)

In Canada, VOx microbolometer arrays have also been in active development since the 1990's.[2] The prime manufacturer, INO, produces high quality arrays with precedence for selection for space applications.[3] Export controls were found to be non-prohibitive but the delivery time for INO's custom arrays could be problematic for imager development cycles less than a year. Currently, the lack of large commercial production is more than compensated by the availability of custom arrays and interest in developing a product for EO.

4.1..3 France (ULIS)

Another noteworthy source of commercial microbolometer arrays can be found in France where the production technology, initiated by the government infrared entity, LETI/LIR in 1992, has since been commercially transferred to industry.[4] These commercial microbolometer arrays have competitive performances with those produced in North America but are based on Amorphous Silicon instead of Vanadium Oxide. The result is arrays with slightly lower responsivities but with significantly lower thermal time constants. This becomes a key parameter when contemplating high GSD from fast moving (~7 km s^{-1}) satellite platforms. The key advantage of the French arrays is their large production line, precedence for prior EO applications,[3] and strategic plan for array improvements on their commercial line.

4.1..4 Australia

The last significant microbolometer legacy explored by the authors is that found in Australia. The Australian Defense and Technology Organization (DTSO) has researched bolometers since the 1950's with significant developments taking place in the 1980's.[5] DTSO then aggressively developed their amorphous silicon based arrays throughout the 1990's. Australian microbolometer technology has found its way to the commercial sector via a US based company, however production is still limited.

4.1..5 Turkey, South Korea, Japan, and UK

Lastly, the authors examined the technology lines in Turkey, South Korea, Japan, and the UK, which have all successfully demonstrated microbolometer technology.[6-9] However, the availability of low-cost commercial arrays is not as prevalent as those from the US, Canada, and France. In some cases, the technology is still in the development phase. In other instances, the applicable production line does not meet basic EO requirements or has been discontinued.

4.1..6 Summary

In summary, the following table has been compiled to illustrate the results of the COTS detector survey.

Vendor	Detector/ Camera Model	Tech Utilized	Array Size	Pixel Pitch	Reported Performance (NETD, τ, etc.)	Production Status; Export Controlled?
Raytheon Commercial Infrared (Texas Instruments)	IR 2000 AS	a-Si	160 x 120	25 um	NETD < 100 mK	In development
	SB-151 (military)*	VOx	320 x 240	50 um	NETD = 25 mK, τ = 18 ms	In production
	AE-189 (commercial)	VOx	320 x 240	50 um	NETD = 90 mK	In production
	SB212	VOx	320 x 240	25 um	NETD < 50 mK	In development
	No model designation	VOx	640 x 480	25 um		In development
BAE SYSTEMS North America	SIM 300L	VOx	160 x 120	46 um	NETD < 75 mK	In production; export controlled
	SIM 300H (MicroIR LTC550)	VOx	320 x 240	46 um	NETD < 26 mK	In production; export controlled
	No model name	VOx	320 x 240	28 um	NETD < 50 mK	Demonstrated
	MicroIR LTC650	VOx	640 x 480	28 um	NETD < 50 mK	Demonstrated
DRS Technologies (Boeing)	**U3000***	VOx	320 x 240	51 um	NETD = 40 – 100 mK	In production
	U4000	VOx	320 x 240	51 um	NETD = 33 mK	In production
	U6000	VOx	640 x 480	25.4 um		Initial production
Indigo Systems Corp.	Merlin	VOx	320x240	51um	< 100 mK	In production; export controlled
	UL3 Alpha	VOx	160x128	51 um		Replaced by the UL3 Omega
	UL3 Omega	VOx	160x128	51 um	< 40 mK	In production; export controlled
FLIR Systems (US)	Thermovision 320 series		320 x 240	?	Not available	In production
Infrared Solutions, Inc. (US)	IR 160	VOx				
INO (Canada)	No model designation	VOx	256 x 1	52 um	NETD < 100 mK	In production
	No model designation	VOx	160 x 120	52 um	NETD = 175 mK	In production
	No model designation	VOx	256 x 40	52 um	?	Custom order
	No model designation*	VOx	512 x 3	39 um	NETD < 80 mK	Custom array; available Jul 04
ULIS (France)	ULIS 01 01	a-Si	320 x 240	45 um	NETD < 100 mK, Response = 6 mV/K	In production; export controlled (~3 month license process)
	ULIS 01 02 1 E	a-Si	320 x 240	45 um	NETD < 240 mK	In production; export controlled
	No model name	a-Si	320 x 240	35 μm	TBD	Future production
	No model name	a-Si	320 x 240	25 μm	TBD	Future production
	No model name	a-Si	640 x 480	35 μm	TBD	Future production

Infrared Components Corporation (Australian Technology)	**MBC Series**	a-Si	320 x 240	?	NETD < 100 mK	In production

Table 1: Results of COTS Detector Survey

5.0 DETECTOR CHOICE

After examining over 32 models from 11 different manufacturers, we have initially settled on a French COTS (ULIS, formally known as Sofradir) 320 x 240 microbolometer array described in the table below.[10] The key rationale being that this array is fairly representative of the state of the art and is readily available within the European academic community. However, as noted in section 2.0, the nature of rapid microsatellite development times supports the insertion of any technology that is deemed appropriate during the initial design phase. For subsequent TIR imager designs, other COTS detector arrays, to include those based on MEMS microcantilever technology, may be selected using the best fit at the time to the selection criteria defined in section 3.0.

Detector Array Parameter	**Value**
Model Name	UL 01 01 1
Manufacturer	ULIS (Grenoble, France)
Detector Type	Microbolometer Detector Array
Detector Material	Resistive Amorphous Silicon
TCR of detector material	2.5 %/K
Design Waveband	8 – 14 μm
Pixel Count	240×320
Pixel Pitch	$45 \ \mu m \times 45 \ \mu m$
Fill Factor	> 80 %
Sensitive area	$11.4 \ mm \times 10.8 \ mm$
Responsivity (mV/K)	4 mV/K
Peak Responsivity (W/K)	7×10^6 V/W
NETD @ 300 K w/ f/1 optics	< 120 mK
Thermal time constant	4 ms (-3 dB cut-off)
Frame Rate	50 – 60 Hz (5.5 MHz clock)
Rms noise	480 μV
Dynamic Range	60 K (-10° C to + 50° C)
Power Consumption	< 200 mW
Weight	< 50 g
Cost	$10,000 Euros

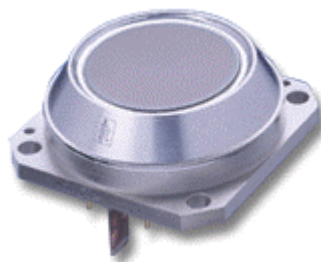Table 2: Parameters of ULIS Microbolometer Array

Figure 2: ULIS 01 01 1 Microbolometer Array

In addition, the array comes integrated with a thermally stabilized Peltier cooler, and read-out integrated circuit. The values for peak responsivity ($\Re$) and rms noise (V_N) were not directly specified but were calculated to be approximately 7×10^6 V/W and 480 μV respectively from the specified parameters. These values are consistent with data found in other previously published reports.[11]

REFERENCES:

1. Kruse, Paul W., *Uncooled Thermal Imaging, Arrays, Systems, and Applications*, SPIE Press 2001.

2. Pope, Jerominek, et. al., "Commercial and Custom 160 x 120, 256 x 1, and 512 x 3 Pixel Bolometric FPAs", *Proceedings of SPIE Vol. 4721*, pp. 64 – 74, 2002.

3. Olivier Saint-Pé, et. al., Study of an Uncooled Focal Plane Array for Thermal Observation of the Earth, *Proceedings of SPIE Vol. 3436*, 1998, pp. 593.

4. Tissot, J. L., et. al., "Technical trends in amorphous silicon based uncooled IR focal plane arrays", *Proceedings of SPIE Vol. 4820*, 2002.

5. Liddiard, Kevin C., "Perspectives of Australian uncooled IR sensor technology", *Proceedings of SPIE Vol. 4130*, 2000.

6. Eminoglu, S., Tanrikulu, M. Y., Tezcan, D. S., Akin, T., "Low-cost, small-pixel uncooled infrared detector for large focal plane arrays using standard CMOS", *Proceedings of SPIE, Vol. 4721, Infrared Detectors and Focal Plane Arrays VII*, p. 111 – 121, 2002.

7. Kim, J. K., Han, H. H., "A new uncooled thermal IR detector using silicon diode micromachined isolated silicon diode for IR detection (MISIR)", *Proceedings of SPIE, Vol. 4130, Infrared Technology and Applications XXVI*, p. 198 – 207, 2000.

8. Tezcan, D. S., et al., "An uncooled microbolometer infrared detector in any standard CMOS technology", *Transducers '99*, p. 610 – 613, 1999.

9. McEwen, R. K., Manning, P., "European Uncooled Thermal Imaging Sensors", *Proceedings of SPIE Vol. 3698, Infrared Technology and Applications XXV*, p. 322 – 337, (1999).

10. Technical Data Package, Reference of the Product: UL 01 01 1, ULIS company document 000/000/28.10.02/039-2/UNT, 2002.

11. Geoffray, Hervé, et. al., *Measured Performance of a Low Cost Thermal Infrared Pushbroom Camera Based on Uncooled Microbolometer FPA for Space Applications*, Proceedings of SPIE Vol. 4540, 2001, pp. 298.

EOARD Grant/Cooperative Agreement Award
Award No. FA8655-03-1-3072
Low-Cost Satellite Infrared Imager Study
University of Surrey Project Ref. 107627
UNIVERSITY OF SURREY DELIVERABLE 2: ATTACHMENT 3 (OF 5)
TASK 3: COMPLETE PRELIMINARY IMAGER DESIGN

1.0 INTRODUCTION

In this attachment, the design methodology adapted for a low-cost thermal infrared (TIR) Earth observation (EO) imager will be summarized. First, the initial assumptions and requirements affecting the design are presented followed by a summary of a basic instrument concept (optics and electronics). Then, the imager's expected performance is analysed using a mathematical radiometric model. Lastly, the issue of instrument calibration is address as well as the larger mission level design, followed by a general assessment of the application of uncooled COTS detector technology to thermal infrared mission areas.

2.0 INITIAL ASSUMPTIONS AND REQUIREMENTS

The primary mission objectives for our TIR imager concept are two-fold and have been derived from the mission analysis presented in attachment 1 of this report. The first objective is to perform useful thermal imaging of the Earth's surface. The instrument should be capable of creating a ground scene map of temperature differences related to spatial flux and emissivity differences across the scene. Potential applications for this mission objective include:

- Sea-surface temperature and sea-ice migration
- Vegatation, hydrological, environmental and urban area change detection

The second key objective is to detect terrestrial hot-spot events. This includes the ability to distinguish, locate, and characterize these events from a nominal Earth scene, day or night. Potential applications for this mission objective include:

- Forest or brush fire detection and monitoring
- Volcanology (predict and monitor eruptions)

These two mission objectives have been chosen, partly because they encompass traditional and emerging thermal infrared imaging mission, but also because they cover the spectrum of potential requirements to be considered at a later time during instrument and satellite constellation customisation. In one set of mission scenarios, thermal imaging, precise noise equivalent temperature difference (NETD) and high spatial resolution become the key parameters for optimization. In the other set, hot-spot detection, a large dynamic range and large ground coverage become more important.

The specific instrument requirements result from iterative analysis of both mission objectives and instrument and imaging platform constraints. The assumed instrument constraints include the detector's radiometric limits, necessary for this low-cost, COTS approach, which are taken from the detector survey. The assumed imaging platform constraints include factors such as orbital geometry, typically subject to the requirements of the primary mission in a "piggy-back" microsatellite launch mode, etc., and size of allowable optics for a typical EO microsatellite platform. These constraints are summarized in the following table:

Baseline Boundary Conditions	Value
Satellite altitude	710 km (typical for sun-synchronous LEO orbit)
approx. weight	1-3 kg
approx. size	10-15 cm^3
approx. power consumption	< 5 W
Interfaces	LVDS – Data out / CAN[1] Control
Optics Speed	f/1 – f/1.5
Detector array size	240 x 320 pixels
Pixel pitch	45 μm
Detector Responsivity	4 mV/K (no atm., 8-14 μm)

Table 1: Baseline constraints for the TIR imager

With the mission objectives and constraints defined, the iterative generation of the remainder of the instrument's requirements was performed. During this process, trade-offs between three primary metrics, 1) thermal sensitivity, 2) spatial resolution, and 3) ground coverage were made. For our instrument, thermal sensitivity could be increased by increasing the amount of scene energy available to the detector, i.e. lowering the f/# or increasing the spectral bandwidth. In the same way, spatial resolution and ground coverage could be increased or decreased by adjusting the imager focal length within the payload size limitations. The sub 8-14 μm wavebands in the table have been chosen based on heritage TIR missions and the inevitable requirement for atmospheric correction, discriminating ground features, and customisation. Taking all these factors into account the following list of requirements was used for the baseline design.

Initial Requirement (selectable)	Value
Imaging mode	Staring array or pushbroom
GSD @ 710 km	500 m
Swath width	160 km (300 km for camera pair)
Candidate spectral channels	8-9, 10-11, 11-12, 8-14 μm
Spatial frequency	> 20 % Nadir MTF @ Nyquist Freq.
Scene temperature range	273 – 333, 500, 800, 1200 K
Temperature accuracy	< 1 K at 300 K

Table 2: Selectable requirements for TIR imager

These requirements have been designed to be flexible at the present. As the instrument takes shape and it's true capabilities become apparent, the generation of firm requirements for a customised mission will become possible.

3.0 INITIAL OPTICS DESIGN

The final optical design will not be defined until after the laboratory test phase of our development cycle. However, a preliminary concept has been laid out given the required

---

[1] CAN – Controller Area Network – a telemetry, telecommand and data communication network supported by certain COTS microprocessors.

point spread function (PSF) and modulation transfer function (MTF) derived from the baseline requirements. For the bench-top prototype, the most liberal requirements were chosen to facilitate a low development cost and a short development timeline. The resultant baseline design is an f/1.1 Petzval objective with a focal length of 60 mm. In order to reduce aberrations, the second surface of each of the two elements is aspherised. For the flight model, the lens material will probably be Germanium and/or Zinc Selenide

4.0 INITIAL ELECTRONICS DESIGN

At the microbolometer pixel level, absorbed incident radiation causes a change in pixel temperature, which, in the case of semiconducting bolometric materials, reduces its electrical resistance. Since the pixel is pulse biased with a set voltage, the resultant change in current signal can be measured by the detector read out integrated circuit (ROIC), which is part of the COTS detector package. After a thermal scene is 'imaged' on the array, the respective signal currents are reduced by a dark pixel current and then integrated into a voltage signal row by row at the bottom of each array column (ripple operation). In turn, all 76,800 pixels are read out as a 5 MHz analogue video signal resulting in a 60 Hz frame rate. One of the key advantages of using a COTS detector is the ease of electrical interfacing via the ROIC. The video output from the ROIC is similar to that found on some of our current imager systems, and so we had made use of our design heritage for image acquisition, storage and downloading.

After leaving the detector ROIC, the analogue video signal enters the Surrey Space Centre (SSC) engineered electronics. The video signal is first digitised to an 8-bit digital stream and then read into a solid-state data-recorder (SSDR). The data is then held until ready for transmission to Earth under the control of a field programmable gate array (FPGA), which links the SSDR to a dedicated downlink. The FPGA also contains all the sequencing and timing logic for system, as well as all the control signals needed to operate the imager under the various data collection scenarios. The command and control of the FPGA is performed by a microcontroller. The microcontroller sends and receives telecommands and telemetry though Control Area Network (CAN) packets from other on-board controllers. It can also provide on-board image processing such as automatic feature detection and data-compression. The downlink speed will depend on the particular host satellite. Typical rates for microsatellites range from 9.6 kbps to a few Mbps.

5.0 EXPECTED PERFORMANCE

Before committing to the expense of prototyping the instrument, it is important to examine a realistic prediction of on-orbit radiometric performance. In the following section, the first mission objective, thermal imaging, will be examined by looking at the expected signal to noise ratio (SNR) as well as the noise equivalent temperature difference (NETD) of a nominal Earth scene. The second mission objective, hot spot detection, will be examined by determining the minimum size of a sub-pixel hot spot required to raise the effective pixel temperature to a given threshold.

5.1 Thermal imaging

For the nominal thermal imaging case, the SNR will first be examined. In microbolometers, there are four primary sources of noise: Johnson noise, 1/f power law noise, temperature fluctuation noise, and background fluctuation noise. For our detector array, the combined noise was calculated to be approximately 480 μV. This value has been confirmed with the detector array vendor. In order to evaluate the SNR for various mission scenarios, the following definition was applied:[1]

$$SNR = \frac{P_I}{P_N} \qquad (1)$$

where P_I is the collected radiant power at the detector pixel and P_N is the detector noise equivalent power (radiant power incident upon a pixel which gives rise to a signal equal to the rms pixel noise within the system bandwidth). Putting P_I in terms of scene temperature/emissivity and taking into account atmospheric and optical losses as well as detector efficiency, the following equation has been derived:

$$SNR = \frac{A_D}{4(f/\#)^2 V_N} \int_{\Delta\lambda} W(\lambda)\Re(\lambda)\tau_O(\lambda)\tau_A(\lambda)d\lambda \qquad (2)$$

where A_D is the detector area, $\Re$ is the detector responsivity in volts per incident watt, τ_O and τ_A are the imager optical and atmospheric transmissions respectively, and W is the thermal irradiance of the ground scene (W/m^2). Since the last four terms are wavelength dependent, their combined effect is integrated across the selected waveband.

In order to calculate the thermal irradiance, Planck's curve for a 300K blackbody was combined with John Hopkins University emissivity data (found in the ASTER Spectral Library version 1.2)[2] and the MODTRAN computer model[3] to model Earth scene radiance across the thermal infrared (8 – 14 μm). Assuming a 75% optical transmission, f/1 optics, 45 μm pixel pitch and 80 % fill factor, and a detector responsivity modelled on the vendor published spectral response and peaking at 7 x 10^6 V/W, the SNR values in table 3 were calculated for the specified wavebands. The SNR values are promising; roughly ½ as much as for the design (terrestrial) use in the 8 – 14 um band and about ⅛ as much in the sub-bands.

Waveband	SNR
8 – 9 μm	63
10 – 11 μm	91
11 – 12 μm	78
8 – 14 μm	364

Table 3: SNR for various thermal imaging wavebands

While these calculations are reassuring, they assume the scene irradiance is much higher than the background. Therefore, it is important to examine the noise equivalent temperature difference (NETD). The NETD is one of the most important figures of merit in any thermal imaging system. In addition, the vendor usually specifies a baseline NETD so it is straightforward to compare candidate detectors. However, NETD is a function of the instrument configuration so an understanding of the vendor's measurements conditions and their relationship with that of a space-borne application is important. Since NETD can be defined as the difference in temperature between two blackbodies of large lateral extent that, when viewed by a thermal imaging system, causes a change in SNR of unity, the following expression can be derived from equation (2). This is done by differentiating with respect to temperature, and setting SNR to one.

$$NETD = \frac{4(f/\#)^2 V_N}{A_D} \left(\int_{\Delta\lambda} \left(\frac{\Delta W(\lambda)}{\Delta T} \right) \tau_O(\lambda)\tau_A(\lambda)\Re(\lambda)d\lambda \right)^{-1} \qquad (3)$$

where V_N, A_D, τ_O, τ_A, and $\Re$ are the same as previously defined. In (3), $(\Delta W(\lambda)/\Delta T)$ represents the change with respect to temperature in the power per unit area emitted by a blackbody at temperature, T, measured with the spectral bandwidth $\Delta\lambda$. In a laboratory environment, at $T = 300$ K and across $8 - 14$ μm, $(\Delta W(\lambda)/\Delta T) = 2.59$ W m^{-2} K^{-1} which, assuming no atmospheric losses, corresponds to the vendor specified NETD of 120 mK. However, we are interested in NETD as it relates to a thermal Earth scene, and so atmospheric effects, as well as sub divided wavebands are factored into (3). The results are listed in the following table:

Waveband	NETD
8 – 9 μm	0.84 K
10 – 11 μm	0.78 K
11 – 12 μm	0.89 K
8 – 14 μm	0.18 K

Table 4: NETD for various thermal imaging wavebands

5.2 Hot spot detection

To evaluate the expected performance for the second prime mission objective (hot spot detection), the incident power collected by a detector pixel will be calculated using the same method as in the previous section. However, the upwelling irradiance will be derived from a 300 K forest ground pixel with a sub-pixel hot spot modelled as 500 K, 800 K, and 1200 K blackbodies respectively.[4] Since the ground pixel has both a hot and cool component, the effective pixel temperature, as seen by the imager, is much lower than if the entire pixel was consumed by the hot spot. Therefore, we have only to determine a threshold "effective" pixel temperature and calculate the corresponding sub-pixel hot spot dimensions. The resultant ground pixel fractions, consumed by a hot spot, for an effective temperature threshold of 320 K in the $8 - 9$ μm and $8 - 14$ μm wavebands are shown below. For completeness, the pixel fractions are also expressed in area for a GSD of 500 m.

Waveband	500 K (Smouldering Fire)	800 K	1200 K (Blazing Fire)
8 – 9 μm	0.048 (109 m)^2	0.011 (53 m)^2	0.0046 (34 m)^2
8 – 14 μm	0.058 (121 m)^2	0.016 (63 m)^2	0.0069 (42 m)^2

Table 5: Fraction of a 300K ground pixel consumed by hot spot that would yield an effective pixel temperature of 320 K

Taking into account atmospheric transmission, the waveband of greatest thermal contrast for hot spot detection is not in the $8 - 14$ μm but is in the $3 - 5$ μm window (mid-wave IR or MWIR), where hot spots are much brighter and the background Earth scene much lower. As a result, most hot spot detection instruments (existing and proposed) known to the authors have been designed to operate in the MWIR. In addition, the MWIR can be a useful channel for the discrimination of false alarms such as those commonly caused by clouds and Sun glints. This has been recently demonstrated by the DLR BIRD spacecraft which utilized the bi-spectral technique (MWIR and TIR) first proposed by Dozier in 1981.[4] Unfortunately, the microbolometer's response in the MWIR, is dramatically lower than in the TIR. The detector vendor claims that interference effects within the high index microbridge may explain the "absorption" weakening in the MWIR. Whether the lower absorption can be wholly compensated by the increased signal contrast will be an area of exploration for the laboratory phase of instrument development. However, current mission design assumptions cannot rely on the availability of a MWIR band. To partly compensate for this, other spectral wavebands will be used such as the visible and near infrared (see next section).

Another issue for hot spot detection is pixel saturation, given the large potential in extremes in scene radiance. The detector electronics allow for adjustment of both the imaging and blind pixel voltage biases to enable adjustment of the dynamic range. Current SSC imagers have the capability to autonomously adjust their dynamic range in real time, and this process is expected to be applicable to this instrument as well. However, some limits in dynamic range and hence hot spot characterization (sub-pixel location and temperature determination) will undoubtedly have to be accepted in light of the low-cost, compact approach.

6.0 PERFORMANCE VERSUS THE REQUIREMENTS

The authors realise the limited applicability of simple performance calculations such as we have presented in this paper to real world space systems. The decision to commit to a given technology and ultimately a detailed spacecraft instrument design is not one to take lightly, given the heavy investments and risks required. However, the preliminary SNR and NETD calculations show promise that a low-cost and compact approach is feasible. Even though the requirements listed in section 4.1 were loosely and liberally defined, it appears we can well satisfy them. In order to confirm our theoretical findings, hardware testing is planned over the next year at SSC.

7.0 MISSION DESIGN

Given the fundamental limits encountered by a low-cost, compact imager, it's performance as a complement to a larger imaging suite becomes important. In this section two potential mission concepts will be briefly presented. The first is for integration on a 90 kg DMC-type microsatellite[5] and the second, and more extreme concept, is integration on a 7 kg nanosatellite platform similar to SNAP-1.[6]

7.1 Typical microsatellite mission

Given the varied specifications required by the multiple owners of the SSTL Disaster Monitoring Constellation (DMC), there are several different versions of the DMC spacecraft. However, the orbital characteristics are all essentially the same; Sun-synchronous with a local time of the ascending node at 10:00 am, at near 700 km altitude. This has been chosen so that between 4 and 8 spacecraft can provide daily coverage at the Equator with 300 – 600 km ground swaths. A typical DMC imager is composed of six push-broom CCD sensors, configured in two banks of three (red, green and NIR), as part of an overall optical bench assembly. Two tri-axial vector magnetometers and four dual-axis sun-sensors are carried in order to determine the attitude of the spacecraft to better than ± 0.25 degrees, however control is relaxed at ±1 degree. For the addition of a TIR channel (also as an imager pair), the baseline spacecraft EO payload would most likely have the following characteristics:

Waveband	GSD	Swath Width
Visible (0.52 – 0.62 μm)	32 m	600 km
NIR (0.76 – 0.9 μm)	32 m	600 km
TIR (8 – 14 μm)	500 m	300 km

Table 6: Potential microsatellite TIR imaging mission

The entire EO payload (3 imager pairs) would weigh less than 10 kg. While a wideband (8-14 μm), 500 m GSD instrument has been used in this example, the TIR channel for a real DMC mission would be customized to accommodate specific mission requirements.

7.2 Typical nanosatellite mission

The second and more radical mission concept that has been studied for TIR EO is the use of a nanosatellite platform. In 2000, Surrey designed and flew the 6.5 kg nanosatellite SNAP-1, which successfully demonstrated the flight of advanced micro-miniature GPS navigation, on-board computing, and propulsion and attitude control technologies.[6] The interface to the CMOS video cameras flown on SNAP-1 would be similar to that which would be used for an integrated TIR EO nanosatellite. Allowing for the additional mass of the TIR imager, the baseline EO payload for a nanosatellite would most likely have the following characteristics:

Waveband	GSD	Swath Width
Visible (0.52 – 0.62 μm)	500 m	150 km
NIR (0.76 – 0.9 μm)	500 m	150 km
TIR (8 – 14 μm)	500 m	150 km

Table 7: Potential nanosatellite TIR imaging mission

7.3 Calibration

One of the key challenges in flying TIR imagers on very small spacecraft is that of instrument calibration. In order to accurately measure ground feature temperatures, reference blackbodies are typically temporarily inserted within the imager field of view to calibrate the effects of inevitable drifts in the imager parameters. Standard practice with heritage systems is to utilize one cold and one hot blackbody to accurately reference the radiometer prior to taking each image. On larger systems, this has been done with the same steering mirror used for image scanning in a wiskbroom configuration. In smaller systems, mechanical arms, mirrors, or paddles are used. In most cases, cold space (3 K) is used as the required cold body and the hot body is on-board the spacecraft bus.

For our systems, calibration schemes can complicate what has been so far a relatively simple and low-cost design. For some mission areas such as those focusing on thermal contrast instead of exact radiometric measurements, on-board calibration may not be required so a non-calibrated system is definitely a consideration for this design. However, one of the advantages of a small, nimble spacecraft is its ability to manoeuvre. The final calibration method is to be determined but heavy emphasis will be given to the use of manoeuvre (spacecraft pan towards cold space) or settling strictly on relative variation mapping with potential cross-calibration with other instruments (such as AATSR). However, consideration will be given to on-board calibration when mission requirements dictate.

8.0 ASSESSMENT: EO AND UN-COOLED TECHNOLOGY

Given the radiometric performance of today's un-cooled infrared detector technology, it has become apparent that they are a valid approach for some TIR EO applications. However, un-cooled technology still holds some basic fundamental limits, which must be realized and accepted before using this approach. One of these limitations is the generally low radiometric response compared to cooled technology. As a result, un-cooled detectors require relatively fast optics. This becomes a major issue when trying to achieve GSDs less than about 250 m from a very small satellite where entrance apertures are limited to approximately 15 to 20 cm or less. Also, a low responsivity means that spectral bandwidths can only be reduced to a certain point. When trying to distinguish scene spectra, a large bandwidth can prove

troublesome. For example, reducing the spectral bandwidth from 4 to 1 µm reduces amount of available scene flux by ¾. For systems where SNR is marginal, this becomes significant.

However, despite these fundamental limits, the advantages of un-cooled technology make them attractive for micro- and nanosatellite developers. In our case, the step to relatively bulky, expensive, and power hungry cryogenically cooled detectors is significant, especially when a potential alternative has yet to be fully discounted. Put simply, the low cost and compact state of commercial un-cooled technology can be the key enabling technology to the flight of a TIR imager on a SSC microsatellite. In the case of very small spacecraft, it is not a question of cooled versus un-cooled but rather, un-cooled or nothing. The ultimate utility for un-cooled TIR detector technology lies in low-cost and highly specialized niche mission areas that benefit greatly from the high temporal resolution offered by satellite constellations. As outlined earlier in this paper, these mission areas are numerous and is expected to grow once a low-cost capability has been established.

Although the un-cooled detector industry has just become ripe for EO mission evaluation, it will only become more so in the future, as the commercial industry continues to improve their products. Some of the future developments already planned include pitch reduction down to 35 µm and array size growth to 640 x 480. This will enable even greater GSD and swath for the same size optics. In addition, reported NETDs are nearing 20 mK and lower. The commercial market for terrestrial TIR cameras has grown tremendously and the small EO satellite stands to profit from this if potential users are prepared to see the advantages.

REFERENCES

1. Riedl, Max J., *Optical Design Fundamentals for Infrared Systems*, SPIE Press, 2001.

2. ASTER Spectral Library Version 1.2, http://speclib.jpl.nasa.gov, JPL, California Institute of Technology, 1998.

3. MODTRAN 3.7 Version 1.0, Air Force Research Laboratory, 11 Nov 1997.

4. Oertel, Dieter, et. al., "Prospective Sensors for Space-borne Fire Observation", *Global and Regional Vegetation Fire Monitoring from Space: planning a Coordinated International Effort*, SPB Academic Publishing bv, 2001.

5. da Silva Curiel, Alex, et. al., "First Results from the Distaster Monitoring Constellation (DMC)", *to be presented at the 2003 IAF Congress*, Bremman, Germany, paper IAA-B4-1302.

6. Underwood, C.I., et. al., "SNAP-1: A Low Cost Modular COTS-Based Nano-Satellite – Design, Construction, Launch and Early Operations Phase", *Proceedings of the 15th Annual AIAA/USU Conference on Small Satellites, SSC01-V-1a, AIAA/ Utah State University*, 2001.

EOARD Grant/Cooperative Agreement Award
Award No. FA8655-03-1-3072
Low-Cost Satellite Infrared Imager Study
University of Surrey Project Ref. 107627
UNIVERSITY OF SURREY FINAL DELIVERABLE: ATTACHMENT 4 (OF 5)
TASK 4: ACQUIRE BASIC COMPONENTS FOR LABORATORY EVALUATION

EQUIPMENT PURCHASED

In support of the subject study, the following hardware/software has been acquired by Surrey Space Centre, University of Surrey:

#		Cost
4		£1,700.00
5	ISOTECH Hyperion Blackbody Source (30 to 80 C)	£2,928.00
6	ISOTECH Gemini R Blackbody Source (30 to 550 C)	£2,729.00
7	ISOTECH Pegasus R Blackbody Source (150 to 1200 C)	£4,134.00
8	ISOTECH VAT*	£1,906.80
9	Land Instruments Cyclops 300AF Portable IR Radiation Thermometer + VAT*	£2,297.00
10	MATLAB, Simulink, Symbolic Math Toolbox (2 ea @ £894)	£1,788.00
11	MATLAB Image Processing Toolbox (2 ea at £192)	£384.00
12	MATLAB Image Acquisition Toolbox (1 ea)	£192.00
13	MATLAB Mapping Toolbox (1 ea)	£192.00
14	MATLAB SimMechanics (1 ea)	£447.00
15	MATLAB VAT*	£525.53
	Total Spent on Equipment	**£34,042.33****

* Current Value Added Tax (VAT) in the UK is 17.5%

**The money committed for equipment comes under the approved amount of £34,276.00 specified in the contract.

VENDORS UTILIZED

The vendors used to purchase the above equipment are as follows:

Item 1: Prolinx Computer Systems, Views Farm Barn, Great Milton, Oxford, OX44 7NW, UK; tel: +44 (0) 1844 279 199; fax: +44 (0) 1844 279 144

Items 2 and 3: CEDIP Infrared Systems, 19 bd Bidault, F-77 183 Croissy-Beaubourg, France; tel: +33 (0) 1 60 37 01 00; fax: +33 (0) 1 64 11 37 55; e-mail: appleshaw@globalnet.co.uk

Item 4: Barr Associates Ltd. Europe, 3 & 4 Home Farm Business Units, Yattendon, Newbury, U.K.; tel: +44 (0) 1635 201317; fax: +44 (0) 1635 202030; e-mail: info@barr-associates-uk.com

Items 5 to 8: Isothermal Technology Ltd., Pine Grove, Southport, Merseyside, PR9 9AG, UK; tel: +44 (0) 1704 543830; fax: +44 (0) 1704 544799; e-mail: info@isotech.co.uk

Items 9: LAND Infrared, Dronfield S18 1DJ, UK; tel: +44+ (0) 1246 417691; fax: +44 (0) 1246 410585; e-mail: infrared.sales@landinst.com

Items 10 to 15: The Mathworks Ltd., Matrix House, Crowley Park, Cambridge, CB4 OHH, UK; tel: +44 (0) 1223 423200; fax: +44 (0) 1223 423289; e-mail: info@mathworks.co.uk

ABSTRACT

A new class of thermal infrared (TIR) Earth Observation (EO) data will become available with the flight of miniature TIR EO instruments in a multiple micro-satellite constellation. This data set will provide a unique service for those wishing to analyse trends or rapidly detect anomalous changes in the TIR characteristics of the Earth's surface or atmosphere (e.g. fire detection). Following a preliminary study of potential mission applications, uncooled commercial-off-the-shelf (COTS) technology was selected to form the basis of a low-cost, compact instrument capable of complementing existing visible and near IR EO capabilities on a sub-100kg Surrey micro-satellite. The preliminary 2-3 kg instrument concept has been designed to yield a 325 m ground sample distance over a 200 km swath width from a constellation altitude of 700 km. The radiometric performance, enhanced with time-delayed integration (TDI), is expected to yield a NETD less than 0.5 K for a 300 K ground scene. Fabrication and characterization of a space-ready instrument is planned for late 2004.

1. INTRODUCTION

The role of space-based Earth Observation (EO) in the thermal infrared (TIR) waveband (8 to 12 μm) has been well demonstrated over the years by numerous missions such as AASTR [1], MODIS [2], BIRD [3], and ETM+ [4]. The user community for such data products is well served and is likely to become more so with further enhancements in (1) radiometric sensitivity or noise equivalent temperature difference (NETD), (2) spatial resolution or ground sample distance (GSD), and (3) ground coverage (revisit time). However, because of the large mission costs and the finite limits of optics size in space, TIR instrument developers typically have to make concessions in one of these factors (GSD, NETD, or revisit time) in order to optimise the other two. As a result, two general classes of TIR EO instruments have emerged as illustrated in Fig. 1. Group 1 is dominated by instruments optimising NETD and spatial resolution at the cost of a decreased revisit time and group 2 is dominated by instruments optimising NETD and ground coverage (revisit time) at the expense of GSD.

This paper proposes a departure from traditional TIR instrument advancement by exploiting the unique capabilities of low-cost EO micro-satellite constellations. Because small EO satellites are limited in their ability to compete directly with existing, larger platforms, they tend to focus instead on reducing the costs of data products or providing niche services currently ill-served. For example, in the visible and near infrared (NIR) wavebands, the four-satellite Disaster Monitoring Constellation (DMC) flown by Surrey Satellites Technology Limited (SSTL) currently provides medium GSD (32 m) full daily coverage of the Earth at a cost below that of a single traditional EO satellite mission [8]. Similarly, with a light-weight and compact TIR EO instrument, a medium GSD (325 m), medium NETD (< 0.5 K), but because of the nature of constellations, a low ground revisit time (2 –3 days) TIR data set will be capable of complementing the already existing DMC imaging products. This potential capability is denoted in Fig. 1 by the circle in the lower-left region of the diagram. While the utility of this data class is still largely unexplored, it would undoubtedly provide a unique service for those wishing to analyse trends or detect anomalous changes in the TIR characteristics of the Earth's surface or atmosphere.
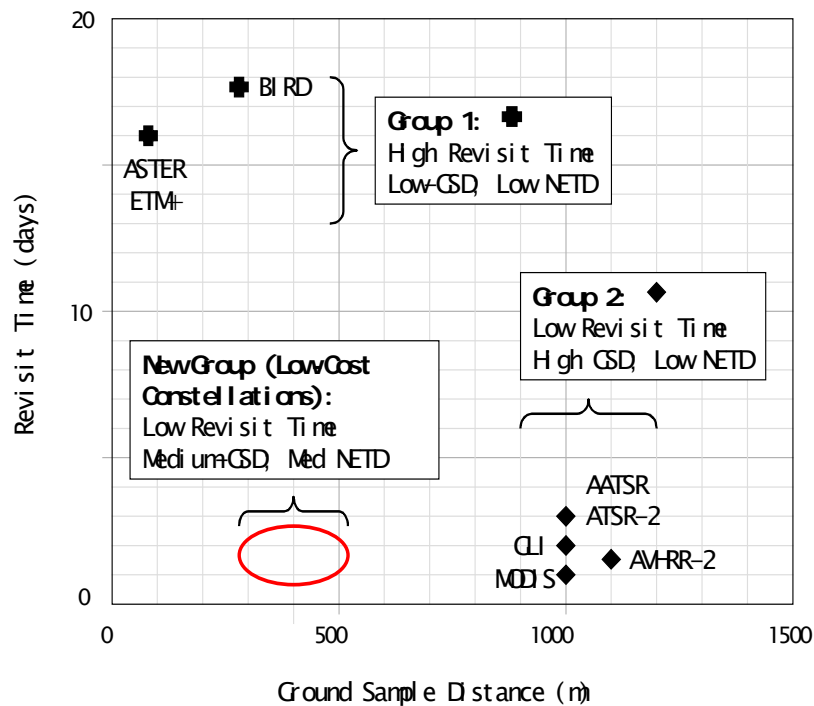
Revisit Time (days) axis: 20, 10, 0

BIRD

Group 1: ✛
High Revisit Time
Low-GSD, Low NETD

ASTER
ETM+

New Group (Low-Cost
Constellations):
Low Revisit Time
Medium-GSD, Med NETD

Group 2: ◆
Low Revisit Time
High GSD, Low NETD

AATSR
ATSR-2
CLI
MODIS◆
AVHRR-2

Ground Sample Distance (m) axis: 0, 500, 1000, 1500

Fig. 1: Ground Revisit Time vs. GSD for several major TIR EO missions [1-7]

In this study, the advantages of small, low-cost satellites have been used as a foundation for the development of a novel miniature TIR EO instrument. In the following sections, a preliminary mission analysis will be presented followed by the instrument concept and its expected performance.

2. MISSION DESIGN

In order to realise this new class of data, our TIR EO instrument needs to be small and light enough to fly on multiple platforms at an affordable cost. However, at the same time the instrument has to be powerful enough (GSD and NETD) to create useful data sets. In order to select the proper balance between these two factors (size/mass and performance), a trade space was bounded by two thresholds. The first threshold is defined by size, mass, and power limits enabling integration into the SSTL DMC imaging suite. The second threshold is defined by TIR EO performance parameters, namely GSD, NETD, and revisit time. The intercept of these two areas defines our trade space for instrument development.

2.1 Microsatellite size/mass/power thresholds

The key contributor to the uniqueness of this proposed TIR EO instrument are the severe mass and size constraints presented by the DMC micro-satellite platform. Although the trend for TIR EO instruments leverages recent advances in the miniaturization of infrared imaging technologies, very few proposed instruments have yet been taken to this extreme. The current limits taken by the TIR EO instrument include those set by DLR's 30 kg BIRD instrument [3] and those proposed by NASA and ESA with the use of uncooled micro-bolometer arrays [9-11]. Although these designs make it possible to fly high-performing TIR (and mid-wave IR) instruments on micro-class satellites (< 100 kg), they would easily consume the entire payload budget for a DMC micro-satellite. Whilst the flight of these instruments in micro-satellite constellations have potential to fill an important TIR EO

niche, it is the focus of Surrey in this study to push TIR EO instrument miniaturization to yet another level. The reasons for doing this are as follows. First, by developing a radically small TIR EO instrument, it can more easily be integrated into the already existing DMC imaging suite. This includes capabilities in medium (32 metre GSD) to medium-high (4 metre) resolution visible and NIR EO. Also, since the TIR is a relatively new development area for Surrey, technological risks can be significantly reduced by starting simple and small much like the earlier development of its current generation of visible and NIR EO capabilities. By slowly introducing TIR to the DMC constellation, the market and utility can be tested at a relatively low cost. Therefore, for this study, the following mass and size thresholds have been determined iteratively with the mission utility thresholds and the instrument design described in the next sections.

Baseline Boundary Conditions	Value
approx. weight	< 2-3 kg
approx. size (optics & detector)	< 2,000 cm^3
approx. power consumption	< 5 W

Tab. 1: Baseline constraints for the TIR imager

2.2 Mission utility thresholds

The second boundary for the trade space are defined by the acceptable levels of GSD and NETD, in light of the increases in revisit time brought by the constellation. Traditionally, spatial (GSD) and radiometric (NETD) resolution requirements for new TIR EO instruments result from an active dialogue and eventual compromise between the user community, who always seeks greater spatial, radiometric, and temporal resolution, and instrument design engineers who determine what is physically and economically feasible. This compromise has solidified over the years and both the user community and instrument developers have since grounded their processes to the capabilities of heritage systems. As a result, somewhat of a departure must be made to validate the new class of data enable by micro-satellite constellations.

Therefore, when evaluating the mission utility of adding a TIR band to DMC, the existing field of TIR requirements has been used as a starting point but has been adapted to exploit the advantages brought by small satellites (reducing costs of existing data sets or providing niche services currently ill-served). The advantages or niche provided by this type of data has been illustrated in Fig. 3. In the upper half of the figure, representative course spatial but high temporal data is compared with more precise spatial but low temporal data (group 1 in Fig. 1). Although the latter data set is much better suited at geo-locating TIR phenomena, the former is better at monitoring the migration of thermal events across the scene.

In the lower half of Fig. 2, course radiometric but high temporal data is compared with precise radiometric but low temporal data (again group 1). In this case, the latter data set is better at determining the surface temperature/emissivity characteristics of the scene. However, the former is much better suited to detect a brief change in scene temperature/ emissivity.

Geolocation of Thermal Event vs. Time

Migration of Thermal Phenomena

Time

Earth Surface Temperature (K) vs. Time

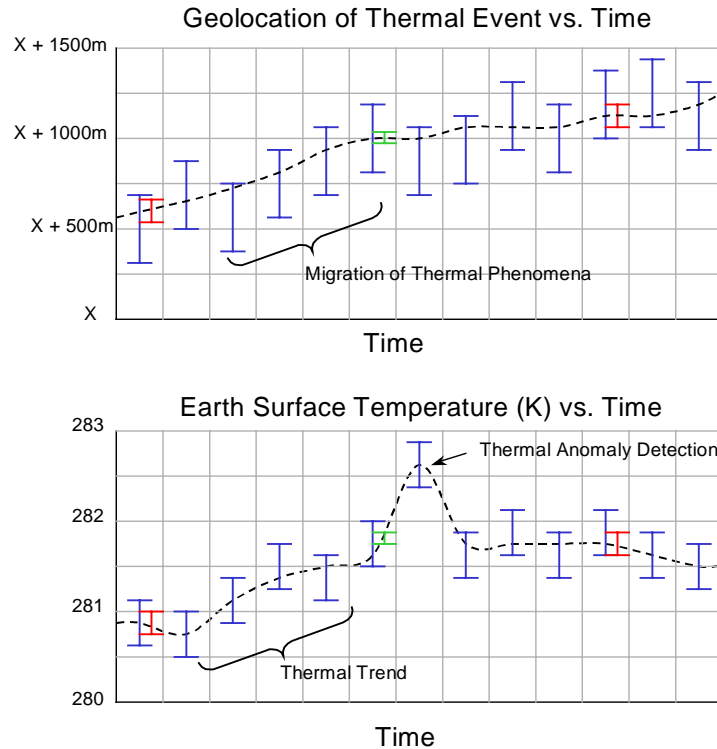Thermal Anomaly Detection

Thermal Trend

Time

Fig. 2: Less precise TIR EO data (spatially and radiometrically) becomes more useful with decreased revisit time

Therefore, in defining suitable mission areas for this new class of compact TIR EO instrument for flight in multi-satellite constellations, two general mission areas were the focus: 1) **analysis of trends**, and 2) **detection of anomalous changes** in the spatial or radiometric characteristics of the TIR signature of the Earth's surface or atmosphere. Development of a sound set of mission applications for this new class of TIR EO data still requires a rigorous dialogue with the user community. However, using a 2003 ESA study (Thermal High-Resolution Earth Mapper - THEMA) reference [12], the following candidate mission applications have served as the starting point for this instrument development:

Mission Application	GSD	NETD	Revisit Time
Thermal Trend Analysis • Forest canopy temp • Crop hydric stress • Volcanic plumes • Costal & marine	300 200 200 300	0.1– 0.3 K 0.1– 0.3 K 0.1– 0.3 K	day day day day
Thermal Change Detection • forest fire detection • volcanic eruptions	200 50	1.5- 2.5K 1.5- 2.5K	1 h week

Tab. 2: Sample Mission application for TIR EO micro-satellite constellations [12]

The THEMA study provides a good starting point because it represents a recent and thorough analysis of user requirements and the general acceptance by the TIR data users. Of special interest is forest fire detection, which, if used in conjunction with on-board detection algorithms and autonomous ground user data transfer, would fill an important niche in the global fire detection community.

2.3 Trade study (size/mass vs. performance)

With the size/weight and utility objectives defined, the iterative generation of the remainder of the instrument's requirements was performed. During this process, trade-offs between performance (GSD, NETD, and revisit time) and estimated size, mass, and power requirements were made. For our instrument, NETD could be decreased by increasing the amount of scene energy available to the detector, i.e. lowering the f/#, increasing the spectral bandwidth, or employing time delayed integration (TDI). In the same way, spatial resolution and ground coverage could be increased or decreased by adjusting the imager focal length within the payload size limitations. The sub 8 - 12 µm wavebands in Tab. 3 have been chosen based on heritage TIR missions and the inevitable requirement for atmospheric correction, discriminating ground features, and customisation (e.g. utilizing a split window technique). Taking all these factors into account the following list of requirements was used for the baseline design.

Initial Requirement (selectable)	Value
Imaging mode	Staring array or pushbroom
GSD @ 700 km	325 m
Swath width	100 km (200 km for camera pair)
Candidate spectral channels	8-9, 10-11, 11-12, 8-14 µm
Spatial frequency	> 20 % Nadir MTF @ Nyquist Freq.
Temperature accuracy	< 0.5 K at 300 K

Tab. 3: Summary of requirements for TIR imager

2.4 Typical microsatellite mission

Given the fundamental limits encountered by a low-cost, compact imager, it's performance as a complement to a larger imaging suite becomes important. In this section a potential mission concept resulting from the integration on a 90 kg DMC-type micro-satellite will be briefly presented. Given the varied specifications required by the multiple owners of DMC, there are several different versions of the DMC spacecraft. However, the orbital characteristics are all essentially the same; Sun-synchronous with a local time of the ascending node at 10:00 am, at near 700 km altitude. This has been chosen so that between 4 and 8 spacecraft can provide daily coverage at the Equator with 300 – 600 km ground swaths. A typical DMC imager is composed of six push-broom CCD sensors, configured in two banks of three (red, green and NIR), as part of an overall optical bench assembly. Two tri-axial vector magnetometers and four dual-axis sun-sensors are carried in order to determine the attitude of the spacecraft to better than ± 0.25 degrees, however control is relaxed at ±1 degree.

For the addition of a TIR channel (also as an imager pair), the baseline spacecraft EO payload would most likely have the following characteristics:

Waveband	GSD	Swath Width
Visible (0.52 – 0.62 μm)	32 m	600 km
NIR (0.76 – 0.9 μm)	32 m	600 km
TIR (8 – 12 μm)	325 m	200 km

Tab. 4: Potential micro-satellite TIR imaging mission

The entire EO payload (3 imager pairs) would weigh less than 10 kg. While a wideband (8 - 12 μm), 325 m GSD instrument has been used in this example, the TIR channel for a real DMC mission would be customized to accommodate specific mission requirements.

3. INSTRUMENT DESIGN

3.1 Cooled vs. uncooled detector technology

The goal in detector selection has been to find candidate commercially available detector array that offer the best performance in terms of weight, size, power consumption, and cost. The TIR EO designer has a variety of cooled technologies to choose from, including ever-shrinking cryo-coolers that are increasingly more power efficient and relatively stable with regards to inducing micro-vibrations. However, in this study, we are looking for an order of magnitude decrease in mass–moving to approximately the 2-3 kg mass range–whilst still achieving reasonable mission utility. Cooled TIR technology may eventually become part of the DMC EO suite, but given reasons outlined in section 2.1, un-cooled detectors have become a practical first step to image in the TIR band.

3.2 Choices in un-cooled technology

In this survey the three main classes of un-cooled infrared technology (pyroelectric, thermoelectric, and resistive bolometer) were initially evaluated. The last class of un-cooled infrared technology, resistive bolometers, has recently been the most aggressively developed of the three for terrestrial applications. Resistive bolometers have been around for decades, but it has been the recent developments in MEMS and thin film technologies that has led to a surge in commercially available micro-bolometer arrays. These arrays are finding multiple markets in fire fighting, security, and manufacturing, which encourages streamlined production processes and increasingly less expensive and better performing devices.

After examining over 32 models from 11 different manufacturers, we have initially settled on a French COTS 320 x 240 amorphous silicon micro-bolometer array on which to base our preliminary design. The array has a pixel pitch of 45 μm with an 80 percent fill factor. The detector response is reported to be 4 mV/K and the thermal time constant is 4 ms. The NETD is given as 120 mK with f/1 optics observing a 300 K target. In addition, the array comes integrated with a thermally stabilized Peltier cooler, and read-out integrated circuit (described in section 3.4). The values for peak responsivity ($\Re$) and rms noise (V_N) were not directly specified but were calculated to be approximately 7×10^6 V/W and 480 μV respectively from the specified parameters. These values are consistent with data found in other previously published reports. [11]

The key rationale this array was chosen was that it is fairly representative of the state of the art and is readily available within the European academic community. However, the nature of rapid micro-satellite development times supports the insertion of any technology that is deemed appropriate during the initial design phase. For subsequent TIR imager designs, other COTS detector arrays may be selected using the best fit at the time.

3.3 Initial optics design

The final optical design will not be defined until after the laboratory test phase of our development cycle. However, a preliminary concept has been laid out given the required point spread function (PSF) and modulation transfer function (MTF) derived from the baseline requirements. For the bench-top prototype, the most liberal requirements were chosen to facilitate a low development cost and a short development timeline. The resultant baseline design is f/1.2 refractive lens triplet with a focal length of 100 mm.

3.4 Initial electronics design

At the micro-bolometer pixel level, absorbed incident radiation causes a change in pixel temperature, which, in the case of semiconducting bolometric materials, reduces its electrical resistance. Since the pixel is pulse biased with a set voltage, the resultant change in current signal can be measured by the detector read out integrated circuit (ROIC), which is part of the COTS detector package. After a thermal scene is 'imaged' on the array, the respective signal currents are reduced by a dark pixel current and then integrated into a voltage signal row by row at the bottom of each array column (ripple operation). In turn, all 76,800 pixels are read out as a 5 MHz analogue video signal resulting in a 50 Hz frame rate. One of the key advantages of using a COTS detector is the ease of electrical interfacing via the ROIC. The video output from the ROIC is similar to that found on some of our current imager systems, and so we had made use of our design heritage for image acquisition, storage and downloading.

After leaving the detector ROIC, the analogue video signal enters the SSTL engineered electronics. The video signal is first digitised to an 12-bit digital stream and then read into a solid-state data-recorder (SSDR). The data is then held until ready for transmission to Earth under the control of a field programmable gate array (FPGA), which links the SSDR to a dedicated downlink. The FPGA also contains all the sequencing and timing logic for system, as well as all the control signals needed to operate the imager under the various data collection scenarios. The command and control of the FPGA is performed by a microcontroller. The microcontroller sends and receives telecommands and telemetry though Control Area Network (CAN) packets from other on-board controllers. It can also provide on-board image processing such as automatic feature detection and data-compression. The downlink speed will depend on the particular host satellite. Typical rates for microsatellites range from 9.6 kbps to a few Mbps.

3.5 Calibration

One of the key challenges in flying TIR imagers on very small spacecraft is that of instrument calibration. In order to accurately measure ground feature temperatures, reference blackbodies are typically temporarily inserted within the imager field of view to calibrate the effects of inevitable drifts in the imager parameters. Standard practice with heritage systems is to utilize one cold and one hot blackbody to accurately reference the radiometer prior to taking each image. On larger systems, this has been done with the same steering mirror used for image scanning in a whiskbroom configuration. In smaller systems, mechanical arms, mirrors, or paddles are used. In most cases, cold space (3 K) is used as the required cold body and the hot body is on-board the spacecraft bus.

For our system, calibration schemes can complicate what has been so far a relatively simple and low-cost design. For some mission areas such as those focusing on thermal contrast instead of exact radiometric measurements, on-board calibration may not be required so a non-calibrated system is definitely a consideration for this design. However, one of the advantages of a small, nimble spacecraft is its ability to manoeuvre. The final calibration method is to be determined but heavy emphasis will be given to the use of manoeuvre (spacecraft pan towards cold space) or settling strictly on relative variation mapping with potential cross-calibration with other instruments (such as AATSR). However, consideration will be given to on-board calibration when mission requirements dictate.

4. EXPECTED PERFORMANCE

Before committing to the expense of prototyping the instrument, it is important to examine a realistic prediction of on-orbit radiometric performance. In the following section, the expected performance will be examined by looking at the expected signal to noise ratio (SNR) as well as the noise equivalent temperature difference (NETD) of a nominal Earth scene. In order to evaluate the SNR for various mission scenarios, the following definition was applied: [13]

$$SNR = \frac{P_I}{P_N} \tag{1}$$

where P_I is the collected radiant power at the detector pixel and P_N is the detector noise equivalent power (radiant power incident upon a pixel which gives rise to a signal equal to the rms pixel noise within the system bandwidth). In micro-bolometers, there are four primary sources of noise: Johnson noise, 1/f power law noise, temperature fluctuation noise, and background fluctuation noise. For our detector array, the combined noise contributed by both the micro-bolometer detector and the electronics was calculated to be approximately 1.4 mV. Putting P_I in terms of scene temperature/emissivity and taking into account atmospheric and optical losses as well as detector efficiency, Eq. 2 has been derived:

$$SNR = \frac{A_D}{4(f/\#)^2 V_N} \int_{\Delta\lambda} W(\lambda)\Re(\lambda)\tau_O(\lambda)\tau_A(\lambda)d\lambda \tag{2}$$

where A_D is the detector area, $\Re$ is the detector responsivity in volts per incident watt, τ_O and τ_A are the imager optical and atmospheric transmissions respectively, and W is the thermal irradiance of the ground scene (W/m^2). Since the last four terms are wavelength dependent, their combined effect is integrated across the selected waveband.

In order to take advantage of the 2-D nature of the detector array and the scanning nature of the orbiting spacecraft, time delay integration (TDI) has been factored into the design. The use of TDI with a 2-D micro-bolometer array in space was successfully demonstrated in 1997 by Goddard Space Flight Center on their Infrared Spectral Imaging Radiometer (ISIR) [9]. With TDI, successive rows of imagery are averaged as they pass over the same scene (see Fig. 4). If applied correctly, matching successive rows exactly, this process has the potential to reduce the SNR by the square of the number of rows used.
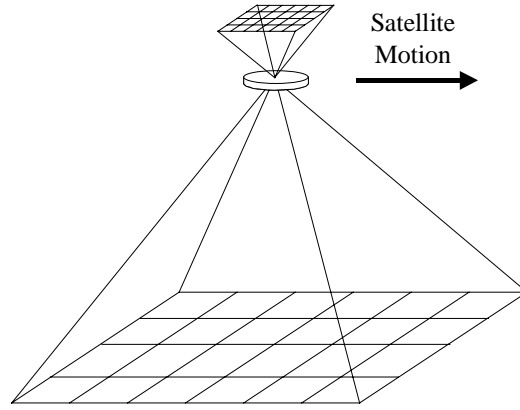
Fig. 4: Application of the 2-D array to perform time-delayed integration (TDI)

So, returning to Eq. 2, Planck's curve for a 300K blackbody was combined with John Hopkins University emissivity data (found in the ASTER Spectral Library version 1.2) [14] and the MODTRAN computer model [15] to model Earth scene radiance across the thermal infrared (8 – 12 µm). Assuming a 75% optical transmission, f/1.2 optics, 45 µm pixel pitch and 80 % fill factor, 1.4 mV of detector and electronics noise, a detector responsivity modelled on the vendor published spectral response and peaking at 7×10^6 V/W, and 50 of the 240 available pixel rows used for TDI, the SNR values in Tab. 6 were calculated for a 300 K ground scene.

Waveband	SNR (TDI 50)
8 – 9 µm	106
10 – 11 µm	153
11 – 12 µm	132
8 – 12 µm	495

Tab. 5: SNR for various thermal imaging wavebands

While these calculations are reassuring, they assume the scene irradiance is much higher than the background. Therefore, it is important to examine the noise equivalent temperature difference (NETD). The NETD is one of the most important figures of merit in any thermal imaging system. In addition, the vendor usually specifies a baseline NETD so it is straightforward to compare candidate detectors. However, NETD is a function of the instrument configuration so an understanding of the vendor's measurements conditions and their relationship with that of a space-borne application is important. Since NETD can be defined as the difference in temperature between two blackbodies of large lateral extent that, when viewed by a thermal imaging system, causes a change in SNR of unity, the following expression can be derived from Eq. 2. This is done by differentiating with respect to temperature, and setting SNR to one.

$$NETD = \frac{4(f/\#)^2 V_N}{A_D} \left(\iint_{\Delta\lambda} \left(\frac{\Delta W(\lambda)}{\Delta T} \right) \tau_O(\lambda) \tau_A(\lambda) \Re(\lambda) d\lambda \right)^{-1} \qquad (3)$$

where V_N, A_D, τ_O, τ_A, and $\Re$ are the same as previously defined. In (3), $(\Delta W(\lambda)/\Delta T)$ represents the change with respect to temperature in the power per unit area emitted by a blackbody at temperature, T, measured with the spectral bandwidth $\Delta\lambda$. In a laboratory environment, at $T = 300$ K and across 8 – 12 μm, $(\Delta W(\lambda)/\Delta T) = 2.59$ W m^{-2} K^{-1} which, assuming no atmospheric losses, corresponds to the vendor specified NETD of 120 mK. However, we are interested in NETD as it relates to a thermal Earth scene, and so atmospheric effects, as well as sub divided wavebands are factored into (3). Taking into account the TDI of 50 pixel rows, the results are listed in Tab. 6:

Waveband	NETD (TDI 50)
8 – 9 μm	0.50 K
10 – 11 μm	0.47 K
11 – 12 μm	0.53 K
8 – 12 μm	0.12 K

Tab. 6: NETD for various thermal imaging wavebands

The authors realise the limited applicability of simple performance calculations such as we have presented in this paper to real world space systems. The decision to commit to a given technology and ultimately a detailed spacecraft instrument design is not one to take lightly, given the heavy investments and risks required. However, the preliminary SNR and NETD calculations show promise that a low-cost and compact approach is feasible. Even though the requirements listed in section 2.3 were loosely and liberally defined, it appears we can well satisfy them. In order to confirm our theoretical findings, hardware testing is planned over the next year at Surrey.

5. ASSESSMENT: EO AND UN-COOLED TECHNOLOGY

Given the radiometric performance of today's un-cooled infrared detector technology, it has become apparent that they are a valid approach for some TIR EO applications. However, un-cooled technology still holds some basic fundamental limits, which must be realized and accepted before using this approach. One of these limitations is the generally low radiometric response compared to cooled technology. As a result, un-cooled detectors require relatively fast optics. This becomes a major issue when trying to achieve GSDs less than about 250 m from a very small satellite where entrance apertures are limited to approximately 15 to 20 cm or less. Also, a low responsivity means that spectral bandwidths can only be reduced to a certain point. When trying to distinguish scene spectra, a large bandwidth can prove troublesome. For example, reducing the spectral bandwidth from 4 to 1 μm reduces amount of available scene flux by ¾. For systems where SNR is marginal, this becomes significant.

However, despite these fundamental limits, the advantages of un-cooled technology make them attractive for micro-satellite developers. In our case, the step to relatively bulky, expensive, and power hungry cryogenically cooled detectors is significant, especially when a potential alternative has yet to be fully discounted. Put simply, the low cost and compact state of commercial un-cooled technology can be the key enabling technology to the integration of a TIR channel(s) in a DMC-like micro-satellite EO constellation. In this, it is not a question of cooled versus un-cooled but rather, un-cooled or nothing. The ultimate utility for un-cooled TIR detector technology lies in low-cost and highly specialized niche mission areas that benefit greatly from the high temporal resolution offered by satellite constellations. As outlined earlier in this paper, this new class of mission areas is expected to grow once a low-cost capability has been established.

Although the un-cooled detector industry has just become ripe for EO mission evaluation, it will only become more so in the future, as the commercial industry continues to improve their products. Some of the developments already coming to market include pitch reduction down to 25 μm and array size growth to 640 x 480. This will enable even greater GSD and swath for the same size optics. In addition, reported NETDs are nearing 20 mK and lower. The commercial market for terrestrial TIR cameras has grown tremendously and the small EO satellite stands to profit from this if potential users are prepared to see the advantages.

6. CONCLUSION

In conclusion, the Surrey Space Centre believes the commercial un-cooled infrared detector array market holds promise for low-cost EO in the TIR. Over the next year, we will be characterizing and testing an imager prototype with the aim of creating novel design options for EO. In the imager development, special emphasis will be given to potential operating in the MWIR, dual channel imaging on the same detector array, and the forest fire detection mission area by parallel development of on-board detection algorithms and autonomous ground user data transfer. It is expected that the same principles applied to the development of low-cost alternatives to the UV, visible, and NIR can be applied to the TIR with fruitful results.

7. ACKNOWLEDGEMENTS

8. DISCLAIMER

The views expressed in this article are those of the authors and do not reflect the official policy or position of the United States Air Force, Department of Defence, or the U.S. Government.

9. REFERENCES

1. AATSR homepage (29 Jan 04):
http://envisat.esa.int/dataproducts/aatsr/

2. MODIS homepage (29 Jan 04): http://modis.gsfc.nasa.gov/

3. DLR BIRD homepage (29 Jan 04): http://spacesensors.dlr.de/SE/bird/

4. NASA ETM+ data page (29 Jan 04):
http://eospso.gsfc.nasa.gov/eos_homepage/mission_profiles/instruments/ETM.php

5. ASTER homepage (29 Jan 04): http://asterweb.jpl.nasa.gov/

6. ADEOS GLI Webpage (29 Jan 04): http://adeos2.hq.nasda.go.jp/shosai_gli_e.htm

7. AVHRR-2 Webpage (29 Jan 04): http://www.eumetsat.de/

8. da Silva Curiel, Alex, et. al., "First Results from the Distaster Monitoring Constellation (DMC)", *presented at the 2003 IAF Congress*, Bremman, Germany, paper IAA-B4-1302.

9. Spinhirne, James D. et. al., "Preliminary Spacecraft Results from the Uncooled ISIR on Shuttle Mission STS-85", http://isir.gsfc.nasa.gov.

10. Saint-Pé, Olivier, et. al., "Study of an uncooled focal plane array for thermal observation for the Earth", *Proceedings of SPIE Vol. 3436*, pp. 593 – 604, 1998.

11. Geoffray, Hervé, et. al., "Measured performance of a low cost thermal infrared pushbroom camera based on uncooled microbolometer FPA for space applications", *Proceedings of SPIE Vol. 4540*, pp. 298 – 308, 2001.

12. Coppo, Peter, et. al., "Requirements and Design of a Thermal High-Resolution Earth Mapper (THEMA) Based on Uncooled Detectors", *Proceedings of SPIE Vol. 4881*, pp. 531 – 542, 2003.

13. Kruse, Paul W., *Uncooled Thermal Imaging, Arrays, Systems, and Applications*, SPIE Press, 2001.

14. ASTER Spectral Library Version 1.2, http://speclib.jpl.nasa.gov, JPL, California Institute of Technology, 1998.

15. MODTRAN 3.7 Version 1.0, Air Force Research Laboratory, 11 Nov 1997.